Dalton Transactions

Accepted Manuscript

ROYAL SOCIETY OF CHEMISTRY

www.rsc.org/dalton

Syntheses, Crystal Structures and Physical Properties of Three New Chalcogenides: $NaGaGe_3Se_8$, $K_3Ga_3Ge_7S_{20}$, and $K_3Ga_3Ge_7Se_{20}$†

Xiaoshuang Li,[abc] Chao Li,[abc] Pifu Gong,[abc] Zheshuai Lin,[ab] Jiyong Yao,[ab,*] and Yicheng Wu[ab]

Three new chalcogenides namely $NaGaGe_3Se_8$, $K_3Ga_3Ge_7S_{20}$, and $K_3Ga_3Ge_7Se_{20}$ of A-Ga-Ge-Q (A = Na, K; Q = S, Se) system were obtained for the first time. They crystallize in two different new structures, albeit both in the monoclinic space group $P2_1/c$. $NaGaGe_3Se_8$ has a layered structure consisting of two dimensional $^{\infty}_{2}[M_4Se_8]^-$ layers separated by Na^+ cations, while the structures of $K_3Ga_3Ge_7Q_{20}$ (Q= S, Se) are constructed by the incompletely isolated quasi-2D $^{\infty}_{2}[M_{10}Q_{21}]^{5-}$ layers, leading to large channels loosely occupied by K^+ cations. Interestingly, thermal analysis indicates that the three title compounds are all congruent-melting compounds, which is uncommon for quaternary compounds and makes bulk crystal growth by

[a] *Center for Crystal Research and Development, Technical Institute of Physics and Chemistry, Chinese Academy of Sciences, Beijing 100190, P.R. China*

[b] *Key Laboratory of Functional Crystals and Laser Technology, Technical Institute of Physics and Chemistry, Chinese Academy of Sciences, Beijing 100190, China, Email: jyao@mail.ipc.ac.cn*

[c] *University of Chinese Academy of Sciences, Beijing 100049, China*

†Electronic supplementary information (ESI) available: Crystallographic data in CIF format for $NaGaGe_3Se_8$, $K_3Ga_3Ge_7S20$, and $K_3Ga_3Ge_7Se_{20}$. CCDC numbers: 1422758-1422760.

Bridgeman technique possible. UV-vis-NIR spectroscopy measurements reveal that the optical band gaps of the three compounds are 2.35, 3.25, and 2.23 eV respectively. In addition, the electronic structure calculation on $NaGaGe_3Se_8$ shows that the band gap mainly determined by the $GaSe_4$ and $GeSe_4$ groups.

Introduction

In recent years, metal chalcogenides have been widely studied owing to their interesting structures and properties.[1-17] Extensive efforts in the synthesis and characterization have led to the discovery of many new metal chalcogenides, including compounds with novel structures such as $AZrPSe_6$ (A = K, Rb, Cs)[18] (having $[ZrPSe_6]^-$ anions with Se−Se bonds), $Ba_4M_2S_8$ (M = Ga, In) [19] (containing the disulfide S_2^{2-} anions), and $Ba_5Ga_4Se_{10}$[20] (possessing the highly anionic $[Ga_4Se_{10}]^{10-}$ cluster with Ga–Ga bond), nonlinear optical (NLO) materials $KPSe_6$,[21] $NaAsSe_2$,[22] ANb_2PSe_{10} (A = K, Rb, and Cs),[23] $BaGa_4Q_7$ (Q = S, Se),[24,25] $SnGa_4Q_7$ (Q = S, Se),[26] $PbGa_4S_7$,[27] and thermoelectric materials $CsBi_4Te_6$,[28] $Ba_3Bi_6MSe_{13}$ (M = Sn, Pb),[29] $Pb_7Bi_4Se_{13}$,[30] $BaCu_{5.9}QTe_6$ (Q = S, Se), [31] etc.

All these findings above can be regarded as significant achievements of synthetic chemistry, which has been enabled by broad-based advances in the understanding of synthesis and characterization methodology. In all synthetic strategies, modification of structures by cation substitution is one of the most important and efficient methods:[32−39] The anionic framework has to arrange in different ways in order to generate commensurate spaces hosting cations with the different sizes, resulting in different structures and the following variation of properties. For example, in the $AAsS_2$ (A = Li, Na)[33] system, the nature of the structure-directing alkali metal ions generates an impressive structural transformation: the polar space group *Cc* of $Li_{1-x}Na_xAsS_2$ holds up to 40% Na, then centrosymmetric phases emerge; the corresponding NLO intensity varies from 10−30 times that of $AgGaSe_2$ to zero finally.

Similarly, in some borates systems, the different coordination environments of alkali metal ions result in the structures changing from noncentrosymmetric types to centrosymmetric ones as well, such as $K_{3-x}Na_xB_6O_{10}Br$ (x = 0.13, 0.67, 1.30, 2.20)[35] and $MCaBe_2B_2O_6F$ (M = Na, K)[37] series. Besides, the smaller ionic radii of Li and Na ions are responsible for the more compact layered structures and the larger SHG effects of $Na_2Be_4B_4O_{11}$[38] and $LiNa_5Be_{12}B_{12}O_{33}$[38], compared with $ABe_2B_3O_7$ (A = K, Rb)[39].

Previously, we reported the synthesis, structure, and physical properties of $LiGaGe_2Se_6$,[3] which crystallizes in the orthorhombic space group *Fdd*2 and shows intriguing nonlinear optical property for mid-IR region. Here, we extend our exploration to the A-Ga-Ge-Q (A = Na, K; Q = S, Se) system, hoping that the larger and also more ionic Na and K cations will have different control over the packing of the anionic structural units from the smaller and more covalent Li atom does, which in turn will help to isolate new phases with interesting stoichiometries, structures, and related properties. Our efforts have led to the discovery of three new members in this family, namely $NaGaGe_3Se_8$, $K_3Ga_3Ge_7S_{20}$, and $K_3Ga_3Ge_7Se_{20}$, which adopt two new structural types different from the $LiGaGe_2Se_6$ structure. In this paper, the syntheses, crystal structures, thermal, optical property, and electronic structure calculations will be reported.

Experimental Section

Reagents

The following reagents were used as obtained: Na (99.9%), K (99.9%), Ga (99.99%), Ge (99.99%), and S (99.9999%), Se (99.9999%), all from Sinopharm. The binary starting materials Na_2S_3, Na_2Se, K_2S_3, K_2Se were prepared by stoichiometric reactions of the elements in liquid NH_3,[40] while Ga_2Q_3 and GeQ_2 were synthesized by the stoichiometric reactions of elements at high temperatures in sealed silica tubes evacuated to 10^{-3} Pa.

Single–crystal growth

Mixtures of A_2S_3 (0.15 mole), Ga_2S_3 (0.15 mole), and GeS_2 (0.60 mole) and A_2Se (0.15 mole), Ga_2Se_3 (0.15 mole), and $GeSe_2$ (0.60 mole) were ground and loaded into fused-silica tubes under an Ar atmosphere in a glove-box, which were sealed under 10^{-3} Pa atmosphere and then placed in a computer-controlled furnace. The samples were heated to 1273 K in 20 h and kept at that temperature for 48 h, then cooled at a slow rate of 2.5 K/h to 573 K, and finally cooled to room temperature. The resultant orange and light-yellow crystals were manually selected for structure characterization. Analyses of eight respective crystals with an EDX-equipped Hitachi S-4800 SEM showed the presence of Na:Ga:Ge:Se in the approximate molar ratio of 1:1:3:8 and K:Ga:Ge:Q in the approximate molar ratio of 3:3:7:20.

Solid–state synthesis

Polycrystalline samples of $NaGaGe_3Se_8$, $K_3Ga_3Ge_7S_{20}$, and $K_3Ga_3Ge_7Se_{20}$ were synthesized by solid–state reaction technique. Mixtures of Na_2Se, Ga_2Se_3, and $GeSe_2$

for $NaGaGe_3Se_8$, K_2Q, Ga_2Q_3, and GeQ_2 for $K_3Ga_3Ge_7Q_{20}$ (Q = S, Se) according to the stoichiometric ratio were ground and loaded into fused silica tubes under an Ar atmosphere in a glovebox, which were sealed under 10^{-3} Pa atmosphere and then placed in a computer-controlled furnace. The samples were heated to 1073 K in 20 h, kept at that temperature for 72 h, and then the furnace was turned off.

X-ray powder diffraction analyses of the powder samples were performed at room temperature in the angular range of 2θ = 10–70 ºwith a scan step width of 0.05 ºand a fixed counting time of 0.2 s/step using an automated Bruker D8 X-ray diffractometer equipped with a diffracted monochromator set for Cu K_α (λ = 1.5418 Å) radiation. Fig. S1 in the ESI† shows XRD patterns of the polycrystalline samples of $NaGaGe_3Se_8$, $K_3Ga_3Ge_7S_{20}$, and $K_3Ga_3Ge_7Se_{20}$ along with the calculated ones on the basis of the single crystal crystallographic data. The experimental patterns are in good agreement with the calculated data.

Structure determination

Single-crystal X-ray diffraction data of $NaGaGe_3Se_8$, $K_3Ga_3Ge_7S_{20}$, and $K_3Ga_3Ge_7Se_{20}$ were collected with the use of graphite-monochromatized Mo Kα (λ = 0.71073 Å) at 153 K on a Rigaku AFC10 diffractometer equipped with a Saturn CCD detector. Crystal decay was monitored by re-collecting 50 initial frames at the end of data collection. The collection of the intensity data, cell refinement and data reduction were carried out with the use of the program Crystalclear.[41] Face-indexed absorption corrections were performed numerically with the use of the program XPREP.[42]

The structures were solved with the direct methods program SHELXS and refined with the least-squares program SHELXL of the SHELXTL.PC suite of programs.[42] Due to the limited ability of X-ray to differentiate the adjacent Ga and Ge, and the very similar bond lengths of all the tetrahedral positions, the Ga and Ge atoms were randomly assigned to the tetrahedral sites according to the ratios determined by EDX measurement in all three compounds. It should be noted that the stoichiometry of the compounds is also proved by the successful stoichiometric synthesis of the pure polycrystalline sample. The final refinement included anisotropic displacement parameters and a secondary extinction correction. Additional experimental details are given in Table 1 and selected metrical data are given in Tables 2, 3, and 4. Further information can be found in supporting information.

Thermal Analysis

A Labsys™TG-DTA16 (SETARAM) thermal analyzer was used to investigate the thermal property by the differential scanning calorimetric (DSC) analysis (the DSC was calibrated with Al_2O_3). About 15 mg of the $NaGaGe_3Se_8$, $K_3Ga_3Ge_7S_{20}$, and $K_3Ga_3Ge_7Se_{20}$ samples were placed in a silica tube (5 mm o.d. × 3 mm i.d.) and subsequently sealed under a high vacuum. The heating and the cooling rates were both 15 K /min.

UV−vis−NIR Diffuse Reflectance Spectroscopy

A Cary 5000 UV-vis-NIR spectrophotometer with a diffuse reflectance accessory was

used to measure the spectra of $NaGaGe_3Se_8$, $K_3Ga_3Ge_7S_{20}$, $K_3Ga_3Ge_7Se_{20}$, and $BaSO_4$ as a reference in the range 250 nm (5.0 eV) to 2500 nm (0.5 eV).

Electronic Structure Calculations

The first-principles calculations for $NaGaGe_3Se_8$ were performed by the plane-wave pseudopotential method implemented in the CASTEP package.[43] Ultra-soft pseudopotentials[44] are chosen and the valence electrons are $2s^2 2p^6 3s^1$ for Na; $3d^{10} 4s^2 4p^1$ for Ga; $4s^2 4p^2$ for Ge; and $4s^2 4p^4$ for Se. In order to calculate the disordered structure, one ordered structure was used in which the sixteen statistical locations were occupied by four Ga and twelve Ge atoms, respectively. The ion-electron interactions were modeled by the ultrasoft pseudopotentials for all elements. The local density approximation (LDA)[45] was adopted to describe the exchange and correlation (XC) potentials. The kinetic energy cutoffs of 350 eV and Monkhorst-Pack *k*-point meshes[46] with a density of (3 × 2 × 1) points in the Brillouin zone were chosen.

Results and Discussion

Crystal structure of $NaGaGe_3Se_8$

As shown in Fig. 1, $NaGaGe_3Se_8$ crystallizes in the centrosymmetric space group $P2_1/c$ of the monoclinic system. There is one crystallographically unique Na atom, four unique metal positions randomly occupied by both Ga and Ge in the molar ratio of 1:3, and eight unique Se atoms in the asymmetric unit, all at general sites 4*e*.

Without Se−Se or metal−metal bonds in the structure, the oxidation states of 1+, 3+, 4+, and 2− can be assigned to Na, Ga, Ge, and Se, respectively.

The basic structure units in $NaGaGe_3Se_8$ are distorted MSe_4 (The M site is randomly occupied by Ga and Ge atoms in 1:3.) tetrahedra (Fig. 1A). In the structure, four MSe_4 tetrahedra are connected by corner-sharing Se atoms to form a M_4Se_{11} group, which is the fundamental building unit of $NaGaGe_3Se_8$ (Fig. 1A). The M_4Se_{11} groups are further connected with each other by sharing Se atoms to form a one-dimensional (1D) $^{\infty}_{1}[M_4Se_{10}]^{5-}$ anionic chain along the *a*-axis (Fig. 1B). The chains then are further linked with each other via sharing edges to generate $^{\infty}_{2}[M_4Se_8]^{-}$ layers (Fig. 1B), which are stacked along the *b*-direction and separated by Na^+ cations (Fig. 1C).

Selected bond distances for $NaGaGe_3Se_8$ are listed in Table 2. The distances of (Ga/Ge)−Se bonds range from 2.3540(19) to 2.4049(18) Å, which are similar to those for tetrahedrally coordinated Ga/Ge atoms in $BaGa_2GeSe_6$ (2.3741(9) to 2.392(1) Å)[47] and $Ga_{16.60}Ge_{0.40}Zn_4Se_{35}$ (2.358(2) to 2.403(2) Å)[48]. As for the Na−Se bond lengths, they are normal, ranging from 2.987(6) to 3.6311(56) Å, which is comparable to those in $NaLnGa_4Se_8$ (Ln = La, Ce, Nd) (3.129(4) to 3.2652(13) Å)[49].

Crystal structure of $K_3Ga_3Ge_7Q_{20}$ (Q = S, Se)

$K_3Ga_3Ge_7Q_{20}$ (Q = S, Se) are isostructural and also crystallize in the centrosymmetric space group $P2_1/c$ of monoclinic system. In the asymmetric unit, there are two crystallographically unique K atoms (Wyckoff sites 2*b* and 4*e*), five metal positions

(Wyckoff sites 4*e*) randomly occupied by both Ga and Ge in the molar ratio of 3:7, and ten unique Q atoms (Wyckoff sites 4*e*). Without Q−Q or metal−metal bonds in the structure, the oxidation states of 1+, 3+, 4+, and 2− can be assigned to K, Ga, Ge, and Q, respectively.

The structures of $K_3Ga_3Ge_7Q_{20}$ (Q = S, Se), taking $K_3Ga_3Ge_7S_{20}$ as an illustration, are shown in Fig. 2. The major structure motif is the corrugated quasi-2D $^{\infty}_{2}[M_{10}S_{21}]^{5-}$ layers (Fig. 2B) constructed by corner sharing $M_{10}S_{26}$ groups (Fig. 2C), which are formed by ten MS_4 (The M site is randomly occupied by Ga and Ge atoms in 3:7.) tetrahedra with corner and edge sharing. The corrugated quasi-2D $^{\infty}_{2}[M_{10}S_{21}]^{5-}$ layers are not completely separated from each other. Rather, they are joined through S10 and S6 atoms, resulting in large channels in the structure. The cross section of the rectangular-shaped channel is about 3.7 x 19.7 $Å^2$. (The radius of M is 0.45 Å.) The K^+ cations are loosely distributed in the channels.

Selected bond distances for $K_3Ga_3Ge_7Q_{20}$ (Q = S, Se) are listed in Tables 3 and 4. For $K_3Ga_3Ge_7S_{20}$, the distances of Ga/Ge−S bonds range from 2.204(2) Å to 2.261(2) Å, which are close to those of 2.208(1) to 2.215(1) Å in $AgGaGeS_4$[50] and 2.246(1) to 2.264(1) Å in $BaGa_2GeS_6$[47]. The K−S bond lengths vary from 3.281(4) to 3.782(4) Å, consistent with those of 3.665(4) to 3.712(2) Å in $KCd_4Ga_5S_{12}$[17], and 3.275(2) to 3.697(2) Å in KBa_2SnS_4Br[51]. For $K_3Ga_3Ge_7Se_{20}$, the lengths of the Ga/Ge−Se bonds range from 2.3333(14) Å to 2.3873(13) Å. These values are comparable to those of 2.3741(9) to 2.392(1) Å in $BaGa_2GeSe_6$[47]. As for the K−Se bond lengths, they vary from 3.418(5) Å to 3.914(6) Å, a bit larger than typical values of 3.352(2) to 3.642(3)

Å in $K_2MnSn_2Se_6$[52], and 3.344(1) to 3.644(1) Å in $K_2Ag_2SnSe_4$[52], although similar values were also found in compounds $KGaSe_2$ (3.264(2) to 3.917(2) Å)[53] and $KBaMSe_3$ (M = As, Sb) (3.315(2) to 3.789(2) Å)[54].

Compared with $LiGaGe_2Se_6$, the dimensions of $NaGaGe_3Se_8$ and $K_3Ga_3Ge_7Q_{20}$ (Q = S, Se) are all reduced as a result of the controlling effect of the larger and more ionic Na and K atoms on the anionic framework. In the structure of $LiGaGe_2Se_6$, the covalency of Li−Se bonds is stronger than those of Na−Se and K−Q bonds and Li atom tends to reside in a slightly distorted tetrahedron with Li−Se varying from 2.64(3) to 2.83(3) Å. Consequently, the small $LiSe_4$ tetrahedra are located in the small cavities of the three-dimensional framework formed by corner-sharing $GaSe_4$ and $GeSe_4$ tetrahedra. Nevertheless, for $NaGaGe_3Se_8$ and $K_3Ga_3Ge_7Q_{20}$ (Q = S, Se), Na and K atoms are coordinated to irregular polyhedra of six or seven Q atoms with Na/K−Q bonds ranging from 2.987(6) to 3.915(6) Å (Fig. 1A and Fig. 2C). Moreover, the Na/K−Q bonds, with their stronger ionic nature and longer distances, have stronger "scissoring" effect in reducing the dimensionality of the structures, resulting in lower dimensional structures (Fig. 1C and Fig. 2A) than $LiGaGe_2Se_6$.

Thermal Analysis

The DSC curves of $NaGaGe_3Se_8$, $K_3Ga_3Ge_7S_{20}$, and $K_3Ga_3Ge_7Se_{20}$ are shown in Fig. 3. It is evident that the title compounds melt congruently at rather low temperatures of ~975/1060/1015 K and recrystallizing at ~960/960/980 K for $NaGaGe_3Se_8$, $K_3Ga_3Ge_7S_{20}$, and $K_3Ga_3Ge_7Se_{20}$ respectively. The congruent-melting behavior of a

chalcogenide material is valuable because it makes the bulk crystal growth by the Bridgman-Stockbarger technique possible. Bulk single crystals are needed for a thorough evaluation and practical application of a material in many cases. Besides, the low-crystal growth temperature and the low Na/K content of the three compounds could also effectively reduce the attacking of Na/K atom to the silica tube, which may provide an additional advantage for the crystal growth.

Optical property

The optical diffuse reflectance method was used for the determination of the band gap. Based on the UV–Vis–NIR diffuse–reflectance spectrum, absorption (F(*R*)) data are calculated from the following Kubelka–Munk function (1):[55, 56]

$$F(R) = \frac{K}{S} = \frac{(1-R)^2}{2R} \quad (1)$$

where *R* is the reflectance, *K* is the absorption, and *S* is the scattering. As shown in Fig. 4, experimental band gaps of the title compounds are 2.35/3.25/2.23 eV for $NaGaGe_3Se_8$, $K_3Ga_3Ge_7S_{20}$, and $K_3Ga_3Ge_7Se_{20}$ respectively.

The band gaps of $NaGaGe_3Se_8$ and $K_3Ga_3Ge_7Se_{20}$ selenides are obviously smaller than that of $K_3Ga_3Ge_7S_{20}$ sulfide. In chalcogenides, the chalcogen atom orbitals usually occupy the top of valence bands and plays the essential role in determining the band gap, the orbitals from cations covalently-bonded with chalcogens usually occupy the bottom of the conduction bands, while orbitals from alkali metal or alkali metal contribute to the bottom of conduction bands in much less degree and affect the band gap indirectly. Because the much lower energy of the S 3*p*

orbitals that that of the Se 4*p* orbitals, the sulfide $K_3Ga_3Ge_7S_{20}$ has the largest band gap among the three. For the two selenides, $NaGaGe_3Se_8$, and $K_3Ga_3Ge_7Se_{20}$, the former has a bit larger band gap than the latter, which may be explained based on the "dimensional reduction" concept, which suggests that lowering the dimensionality of the structure can help to increase the band gap. As the $^{\infty}_{2}[M_4Se_8]^{-}$ layer is completely separated in $NaGaGe_3Se_8$, while corrugated quasi-2D $^{\infty}_{2}[M_{10}S_{21}]^{5-}$ layers are not completely isolated in $K_3Ga_3Ge_7Se_{20}$, leading to its higher structural dimensionality and hence a bit smaller band gap. These interesting interactions indicate that the bonding characteristics could be exploited in band gap engineering to produce compounds with specific optical properties.

Electronic Structure Calculations

The partial density of state (PDOS) projected on the constitutional atoms of $NaGaGe_3Se_8$ is shown in Fig. 5, from which several electronic characteristics are shown: (i) The valence band (VB) lower than -10eV are mainly consisted of the isolated inner-shell orbitals of Na 3s2*p*, Ga 4*s3d* and the 4*s* orbitals of Ge and Se, which have little interaction with neighbor atoms; (ii) The upper part of VB and the bottom of CB are mainly composed of the 4*p* orbitals of Ga, Ge and Se, thus the states on the both sides of the band gap mostly consist of those from the $GaSe_4$ and $GeSe_4$ groups.

Conclusions

Three new chalcogenides namely $NaGaGe_3Se_8$, $K_3Ga_3Ge_7S_{20}$, and $K_3Ga_3Ge_7Se_{20}$ have been obtained. In the structures, the MQ_4 tetrahedra are all connected to each other by corner/edge-sharing to form two-dimensional layers. However, the obvious difference between $NaGaGe_3Se_8$ and $K_3Ga_3Ge_7Q_{20}$ is that, for $NaGaGe_3Se_8$, the $^{\infty}_{2}[M_4Se_8]^-$ layers are completely separated by Na^+ cations, while for $K_3Ga_3Ge_7Q_{20}$, the corrugated quasi-2D $^{\infty}_{2}[M_{10}Q_{21}]^{5-}$ layers are not completely isolated from each other, giving rise to the appearance of large channels occupied loosely by K^+ cations. Additionally, they are all congruent-melting compounds and the optical band gaps of the three compounds are 2.35, 3.25, and 2.23 eV respectively. Such three compounds, with their interesting structures and properties, may arouse further interest in exploring new materials by modifying structures.

Acknowledgments

This research was supported the National Natural Science Foundation of China (No.s 51472251, 21271178).

References

1 Y. Dong, J. Do and H. Yun, *Anorg. Allg. Chem*. 2009, **635**, 2676.

2 S.-M. Kuo, Y.-M. Chang, I. Chung, J.-I. Jang, B.-H. Her, S.-H. Yang, J. B. Ketterson, M. G. Kanatzidis and K.-F. Hsu, *Chem. Mater.* 2013, **25**, 2427.

3 D. Mei, W. Yin, K. Feng, Z. Lin, L. Bai, J. Yao and Y. Wu, *Inorg. Chem*. 2012, **51**, 1035.

4 C. D. Morris, H. Li, H. Jin, C. D. Malliakas, J. A. Peters, P. N. Trikalitis, A. J. Freeman, B. W. Wessels and M. G. Kanatzidis, *Chem. Mater.* 2013, **25**, 3344.

5 W. Yin, W. Wang, L. Kang, Z. Lin, K. Feng, Y. Shi, W. Hao, J. Yao and Y. Wu, *Solid State Chem*. 2013, **202**, 269.

6 Q. Tan, L.-D. Zhao, J.-F. Li, C.-F. Wu, T.-R. Wei, Z.-B. Xing and M. G. Kanatzidis, *J. Mater. Chem. A* 2014, **2**, 17302.

7 P. Yu, L. J. Zhou and L. Chen, *J. Am. Chem. Soc.* 2012, **134**, 2227.

8 W. Yin, K. Feng, W. Wang, Y. Shi, W. Hao, J. Yao and Y. Wu, *Inorg. Chem*. 2012, **51**, 6860.

9 K. Feng, X. Jiang, L. Kang, W. Yin, W. Hao, Z. Lin, J. Yao, Y. Wu and C. Chen, *Dalton Trans.* 2013, **42**, 13635.

10 G. Tan, F. Shi, J. W. Doak, H. Sun, L.-D. Zhao, P. Wang, C. Uher, C. Wolverton, V. P. Dravid and M. G. Kanatzidis, *Energy Environ. Sci.* 2015, **8**, 267.

11 S. M. Islam, S. Vanishri, H. Li, C. C. Stoumpos, J. A. Peters, M. Sebastian, Z. Liu, S. Wang, A. S. Haynes, J. Im, A. J. Freeman, B. Wessels and M. G. Kanatzidis, *Chem. Mater.* 2015, **27**, 370.

12 A. Banerjee, B. D. Yuhas, E. A. Margulies, Y. Zhang, Y. Shim, M. R. Wasielewski and M. G. Kanatzidis, *J. Am. Chem. Soc.* 2015, **137**, 2030.

13 G. Tan, L. D. Zhao, F. Shi, J. W. Doak, S. H. Lo, H. Sun, C. Wolverton, V. P. Dravid, C. Uher and M. G. Kanatzidis, *J. Am. Chem. Soc.* 2014, **136**, 7006.

14 M. Sturza, C. D. Malliakas, D. E. Bugaris, F. Han, D. Y. Chung and M. G. Kanatzidis, *Inorg. Chem.* 2014, **53**, 12191.

15 H. Lin, L. Chen, L. J. Zhou and L. M. Wu, *J. Am. Chem. Soc.* 2013, **135**, 12914.

16 H. Li, C. D. Malliakas, J. A. Peters, Z. Liu, J. Im, H. Jin, C. D. Morris, L.-D. Zhao, B. W. Wessels, A. J. Freeman and M. G. Kanatzidis, *Chem. Mater.* 2013, **25**, 2089.

17 H. Lin, L.-J. Zhou and L. Chen, *Chem. Mater.* 2012, **24**, 3406.

18 S. Banerjee, C. D. Malliakas, J. I. Jang, J. B. Ketterson and M. G. Kanatzidis, *J. Am. Chem. Soc.* 2008, **130**, 12270.

19 J. W. Liu, P. Wang and L. Chen, *Inorg. Chem.* 2011, **50**, 5706.

20 W. Yin, D. Mei, K. Feng, J. Yao, P. Fu and Y. Wu, *Dalton Trans.* 2011, **40**, 9159.

21 A. S. Haynes, F. O. Saouma, C. O. Otieno, D. J. Clark, D. P. Shoemaker, J. I. Jang and M. G. Kanatzidis, *Chem. Mater.* 2015, **27**, 1837.

22 T. K. Bera, J. I. Jang, J.-H. Song, C. D. Malliakas, A. J. Freeman, J. B. Ketterson and M. G. Kanatzidis, *J. Am. Chem. Soc.* 2010, **132**, 3484.

23 J. C. Syrigos, D. J. Clark, F. O. Saouma, S. M. Clarke, L. Fang, J. I. Jang and M. G. Kanatzidis, *Chem. Mater.* 2015, **27**, 255.

24 X. Lin, G. Zhang and N. Ye, *Cryst. Growth & Des.* 2009, **9**, 1186.

25 J. Yao, D. Mei, L. Bai, Z. Lin, W. Yin, P. Fu and Y. Wu, *Inorg. Chem*. 2010, **49**, 9212.

26 Z.-Z. Luo, C.-S. Lin, H.-H. Cui, W.-L. Zhang, H. Zhang, Z.-Z. He and W.-D. Cheng, *Chem. Mater.* 2014, **26**, 2743.

27 X. Li, L. Kang, C. Li, Z. Lin, J. Yao and Y. Wu, *J. Mater. Chem. C* 2015, *3*, 3060.

28 D. Y. Chung, C. Uher and M. G. Kanatzidis, *Chem. Mater.* 2012, **24**, 1854.

29 Y. C. Wang and F. J. DiSalvo, *Chem. Mater.* 2000, **12**, 1011.

30 A. Olvera, G. Shi, H. Djieutedjeu, A. Page, C. Uher, E. Kioupakis and P. F. Poudeu, *Inorg. Chem*. 2015, **54**, 746.

31 M. Oudah, K. M. Kleinke and H. Kleinke, *Inorg. Chem*. 2015, **54**, 845.

32 T. K. Bera, J. I. Jang, J. B. Ketterson and M. G. Kanatzidis, *J. Am. Chem. Soc.* 2009, **131**, 75.

33 T. K. Bera, J. H. Song, A. J. Freeman, J. I. Jang, J. B. Ketterson and M. G. Kanatzidis, *Angew. Chem*. 2008, **47**, 7828.

34 M. S. Devi and K. Vidyasagar, *J. Chem. Soc., Dalton Trans.* 2002, 2092.

35 S. Han, Y. Wang, S. Pan, X. Dong, H. Wu, J. Han, Y. Yang, H. Yu and C. Bai, *Cryst. Growth & Des.* 2014, **14**, 1794.

36 P. F. P. Poudeu, N. Takas, C. Anglin, J. Eastwood and A. Rivera, *J. Am. Chem. Soc*. 2010, **132**, 5751.

37 H. Huang, J. Yao, Z. Lin, X. Wang, R. He, W. Yao, N. Zhai and C. Chen, *Chem. Mater.* 2011, **23**, 5457.

38 H. Huang, L. Liu, S. Jin, W. Yao, Y. Zhang and C. Chen, *J. Am. Chem. Soc.* 2013,

135, 18319.

39 S. Wang, N. Ye, W. Li and D. Zhao, *J. Am. Chem. Soc.* 2010, **132**, 8779.

40 S. A. Sunshine, D. Kang, J. A. Ibers, *J. Am. Chem. Soc.* 1987, **109**, 6202.

41 CrystalClear. Rigaku Corporation: Tokyo, Japan, 2008.

42 G. M. Sheldrick, *Acta Crystallogr. A* 2008, **64**, 112.

43 S. J. Clark, M. D. Segall, C. J. Pickard, P. J. Hasnip, M. J. Probert, Refson, K. M. C. Payne, *Z. Kristallogr.* 2005, **220**, 567.

44 D. Vanderbilt, *Phys. Rev. B* 1990, **41**, 7892.

45 W. Kohn, L. J. Sham, *Phys. Rev.* 1965, **140**, 1133.

46 H. J. Monkhorst, J. D. Pack, *Phys. Rev. B* 1976, **13**, 5188.

47 W. Yin, K. Feng, R. He, D. Mei, Z. Lin, J. Yao and Y. Wu, *Dalton Trans.* 2012, **41**, 5653.

48 T. Wu, X. Wang, X. Bu, X. Zhao, L. Wang and P. Feng, *Angew. Chem., Int. Ed.*, 2009, **48**, 7204.

49 A. Choudhury and P. K. Dorhout, *Inorg. Chem.* 2008, **47**, 3603.

50 J. Rame, B. Viana, Q. Clement, J. M. Melkonian and J. Petit, *Cryst. Growth & Des.* 2014, **14**, 5554.

51 C. Li, K. Feng, H. Tu, J. Yao and Y. Wu, *J. Solid State Chem.* 2015, **227**, 104.

52 X. Chen, X. Y. Huang, A. H. Fu, J. Li, L. D. Zhang and H. Y. Guo, *Chem. Mater.* 2000, **12**, 2385.

53 K. Feng, D. Mei, L. Bai, Z. Lin, J. Yao and Y. Wu, *Solid State Sci.* 2012, **14**, 1152.

54 W. Yin, K. Feng, L. Kang, B. Kang, J. Deng, Z. Lin, J. Yao and Y. Wu, *J. Alloys*

Compd. 2014, **617**, 287.

55 P. Kubelka and F. Munk, *Z. Tech. Phys.*, 1931, **12**, 593.

56 J. Tauc, *Mater. Res. Bull.*, 1970, **5**, 721.

Fig. captions

Fig. 1. (A) Coordination environments of all cations in $NaGaGe_3Se_8$. (B) A single 2D $^{\infty}_{2}[M_4Se_8]^-$ layer perpendicular to the *b* direction with a single M_4Se_{11} group marked by a red circle. (C) Crystal packing structure of $NaGaGe_3Se_8$ viewed down the *a*-axis with the unit cell marked.

Fig. 2. (A) Crystal packing structure of $K_3Ga_3Ge_7S_{20}$ viewed down the *b*-axis with the unit cell marked. (B) A single corrugated quasi-2D $^{\infty}_{2}[M_{10}S_{21}]^{5-}$ layer perpendicular to the *b* direction with a single $M_{10}S_{26}$ group marked by a red circle. (C) A single $M_{10}S_{26}$ group.

Fig. 3. The DSC patterns of $NaGaGe_3Se_8$, $K_3Ga_3Ge_7S_{20}$, and $K_3Ga_3Ge_7Se_{20}$. A: $NaGaGe_3Se_8$, B: $K_3Ga_3Ge_7S_{20}$, C: $K_3Ga_3Ge_7Se_{20}$.

Fig. 4. Optical reflectance spectrum of $NaGaGe_3Se_8$, $K_3Ga_3Ge_7S_{20}$, and $K_3Ga_3Ge_7Se_{20}$. Red: $NaGaGe_3Se_8$, Green: $K_3Ga_3Ge_7S_{20}$, Blue: $K_3Ga_3Ge_7Se_{20}$.

Fig. 5. The total and partial density of states (DOS and PDOS, respectively) of $NaGaGe_3Se_8$. Dashed line represents the Fermi energy (E_f).

Table 1. Crystal data and structure refinements for $NaGaGe_3Se_8$, $K_3Ga_3Ge_7S_{20}$, and $K_3Ga_3Ge_7Se_{20}$.

	$NaGaGe_3Se_8$	$K_3Ga_3Ge_7S_{20}$	$K_3Ga_3Ge_7Se_{20}$
Fw	579.80	1475.79	2413.79
a(Å)	7.2329(14)	6.7665(4)	7.0520(4)
b(Å)	11.889(2)	37.527(2)	39.033(2)
c(Å)	17.550(4)	6.6796(4)	6.9488(4)
β(°)	101.75(3)	90.802(5)	90.433(5)
Space group	$P2_1$/c	$P2_1$/c	$P2_1$/c
V(Å^3)	1477.5(5)	1695.94(18)	1912.67(19)
Z	4	2	2
T(K)	153(2)	153(2)	153(2)
λ (Å)	0.71073	0.71073	0.71073
ρ_c(g/cm^3)	4.235	2.890	4.191
μ(cm^{-1})	27.542	10.053	26.854
$R(F)$ [a]	0.0664	0.0564	0.0502
$R_w(F_o^2)$ [b]	0.1145	0.1156	0.1160

[a] $R(F) = \sum||F_o|-|F_c||/\sum|F_o|$ for $F_o^2 > 2\sigma(F_o^2)$. [b] $R_w(F_o^2) = \{\sum[w(F_o^2 - F_c^2)^2] / \sum wF_o^4\}^{1/2}$ for all data. $w^{-1} = \sigma^2(F_o^2) + (zP)^2$, where $P = (\mathrm{Max}(F_o^2, 0) + 2F_c^2)/3$

Table 2. Selected bond lengths (Å) for $NaGaGe_3Se_8$.

Na–Se1	2.987(6)	Ga/Ge2–Se5	2.3656(19)
Na–Se2	3.023(6)	Ga/Ge2–Se6	2.3540(19)
Na–Se4	3.211(7)	Ga/Ge2–Se7	2.4049(18)
Na–Se5	3.000(6)	Ga/Ge3–Se2	2.3808(19)
Na–Se7	3.6311(56)	Ga/Ge3–Se3	2.3783(17)
Na–Se8	3.2504(70)	Ga/Ge3–Se4	2.363(2)
Ga/Ge1–Se1	2.3863(18)	Ga/Ge3–Se8	2.3636(19)
Ga/Ge1–Se5	2.3785(18)	Ga/Ge4–Se1	2.366(2)
Ga/Ge1–Se6	2.3767(19)	Ga/Ge4–Se2	2.3793(16)
Ga/Ge1–Se8	2.4025(18)	Ga/Ge4–Se3	2.3772(19)
Ga/Ge2–Se4	2.3763(18)	Ga/Ge4–Se7	2.3604(18)

Table 3. Selected bond lengths (Å) for $K_3Ga_3Ge_7S_{20}$.

K1–S1	3.648(4)	Ga/Ge2–S7	2.228(2)
K1–S6	3.707(4)	Ga/Ge2–S8	2.234(2)
K1–S6	3.782(4)	Ga/Ge2–S8	2.246(2)
K1–S7	3.346(4)	Ga/Ge3–S2	2.204(2)
K1–S9	3.337(4)	Ga/Ge3–S3	2.2066(19)
K1–S9	3.398(4)	Ga/Ge3–S7	2.220(2)
K1–S10	3.281(4)	Ga/Ge3–S9	2.226(2)
K2–S3 ×2	3.398(2)	Ga/Ge4–S1	2.227(2)
K2–S4 ×2	3.484(2)	Ga/Ge4–S5	2.217(2)
K2–S8 ×2	3.6117(19)	Ga/Ge4–S6	2.227(2)
Ga/Ge1–S1	2.234(2)	Ga/Ge4–S9	2.2516(19)
Ga/Ge1–S2	3.2455(19)	Ga/Ge5–S5	2.216(2)
Ga/Ge1–S3	3.2406(19)	Ga/Ge5–S6	2.238(2)
Ga/Ge1–S4	2.261(2)	Ga/Ge5–S10	2.213(2)
Ga/Ge2–S4	2.2084(18)	Ga/Ge5–S10	2.216(26

Table 4. Selected bond lengths (Å) for $K_3Ga_3Ge_7Se_{20}$.

K1–Se1	3.914(6)	Ga/Ge2–Se7	2.3601(14)
K1–Se6	3.869(6)	Ga/Ge2–Se8	2.3661(15)
K1–Se6	3.880(6)	Ga/Ge2–Se8	2.3731(16)
K1–Se7	3.430(5)	Ga/Ge3–Se2	2.3333(14)
K1–Se9	3.440(5)	Ga/Ge3–Se3	2.3382(14)
K1–Se9	3.527(6)	Ga/Ge3–Se7	2.3539(16)
K1–Se10	3.418(5)	Ga/Ge3–Se9	2.3660(14)
K2–Se3 ×2	3.5392(11)	Ga/Ge4–Se1	2.3570(15)
K2–Se4 ×2	3.6225(14)	Ga/Ge4–Se5	2.3509(14)
K2–Se8 ×2	3.7194(11)	Ga/Ge4–Se6	2.3615(17)
Ga/Ge1–Se1	2.3607(15)	Ga/Ge4–Se9	2.3873(13)
Ga/Ge1–Se2	3.3704(15)	Ga/Ge5–Se5	2.3484(13)
Ga/Ge1–Se3	3.3665(15)	Ga/Ge5–Se6	2.3721(14)
Ga/Ge1–Se4	2.3841(15)	Ga/Ge5–Se10	2.3409(16)
Ga/Ge2–Se4	2.3518(13)	Ga/Ge5–Se10	2.3439(16)

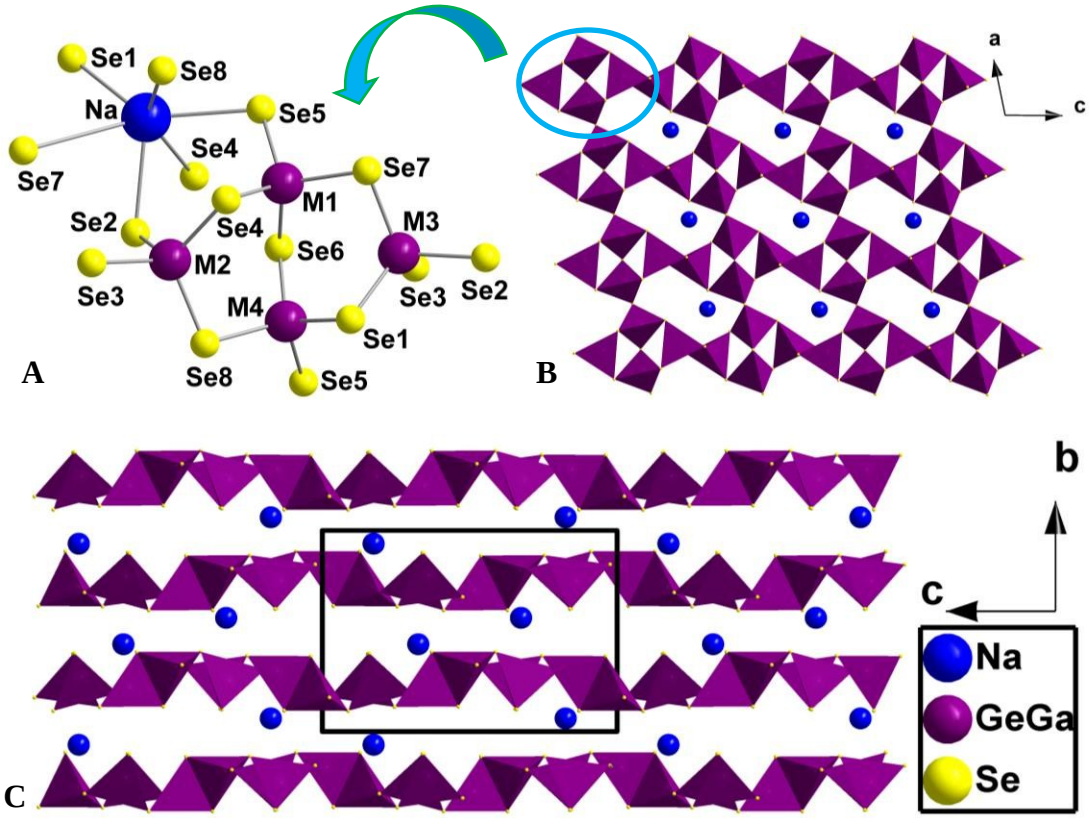

Fig. 1. (A) Coordination environments of all cations in $NaGaGe_3Se_8$. (B) A single 2D $^{\infty}_{2}[M_4Se_8]^-$ layer perpendicular to the *b* direction with a single M_4Se_{11} group marked by a red circle. (C) Crystal packing structure of $NaGaGe_3Se_8$ viewed down the *a*-axis with the unit cell marked.

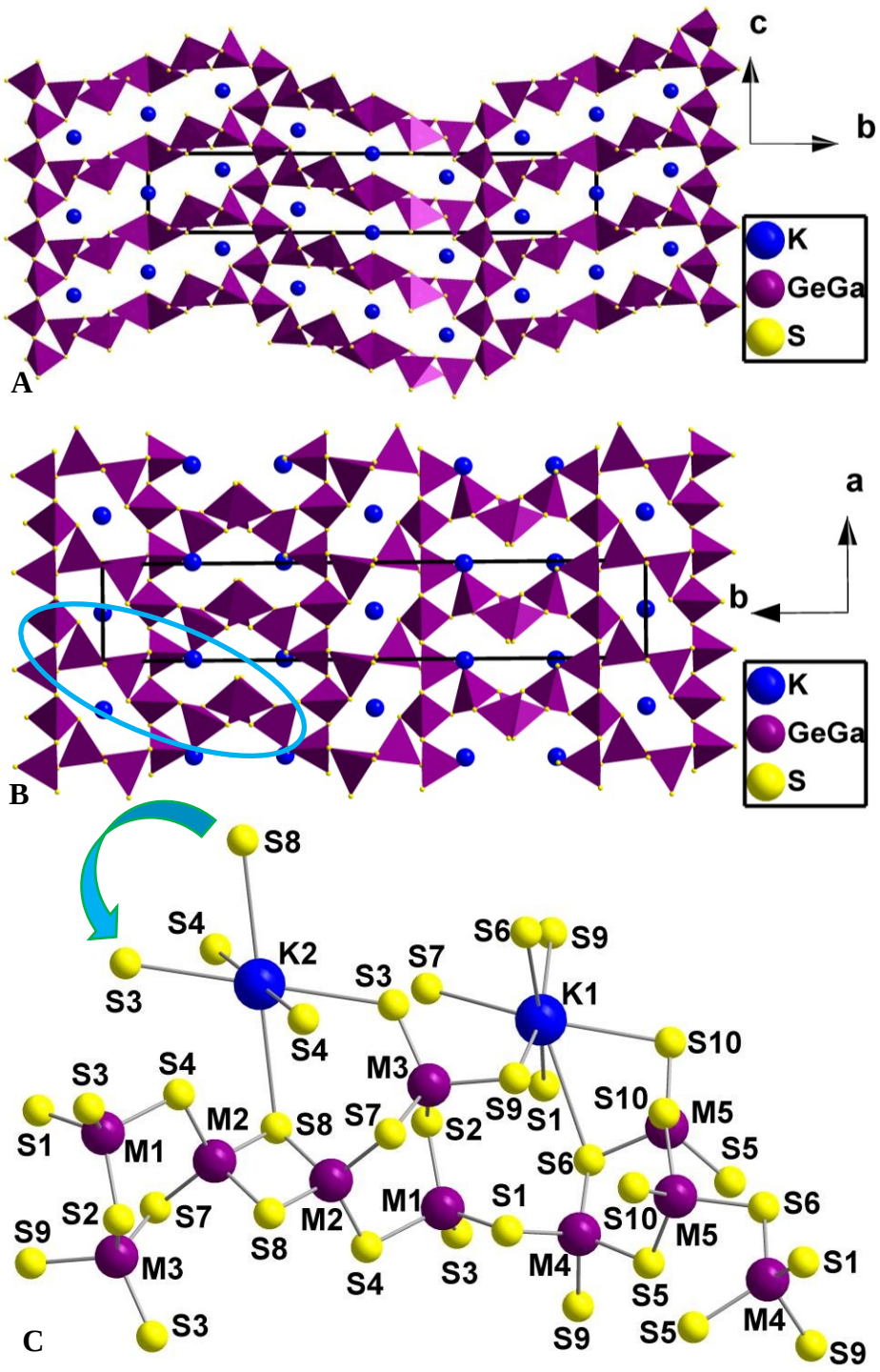

Fig. 2. (A) Crystal packing structure of $K_3Ga_3Ge_7S_{20}$ viewed down the *b*-axis with the unit cell marked. (B) A single corrugated quasi-2D $^{\infty}_{2}[M_{10}S_{21}]^{5-}$ layer perpendicular to the *b* direction with a single $M_{10}S_{26}$ group marked by a red circle. (C) A single $M_{10}S_{26}$ group.

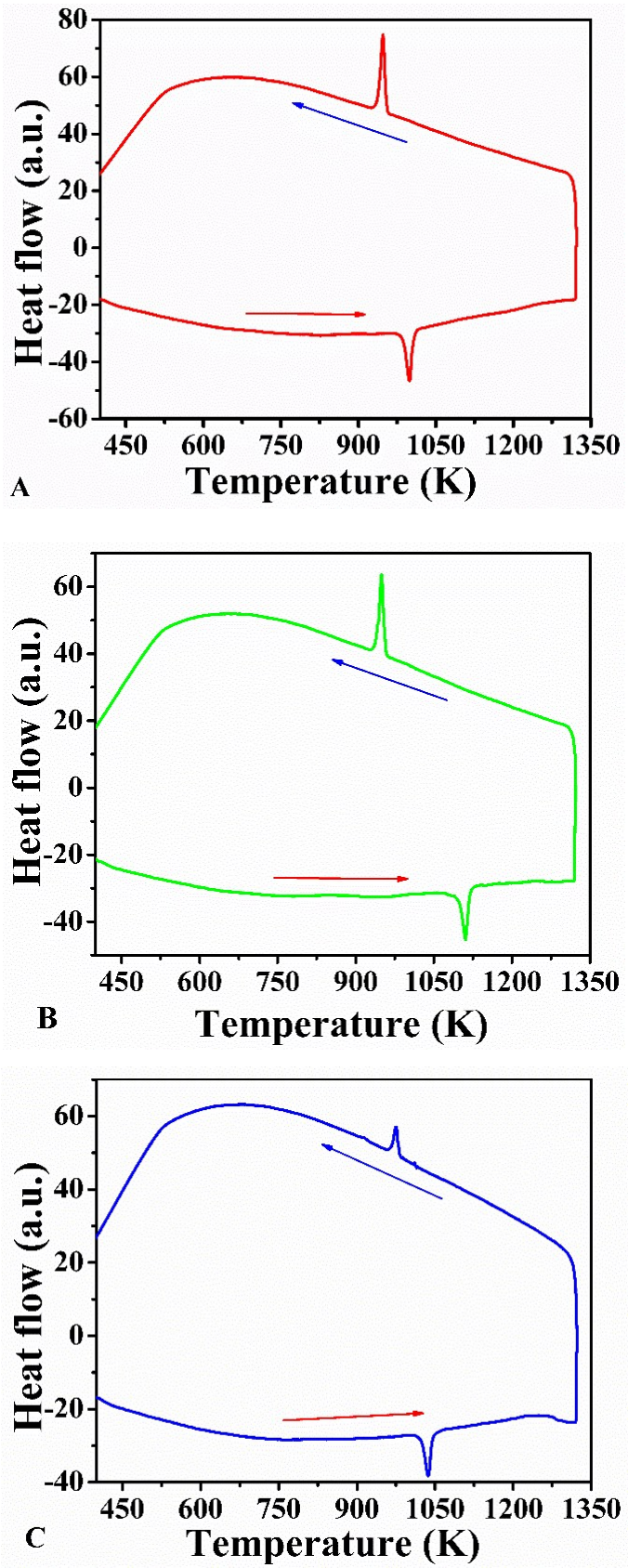

Fig. 3. The DSC patterns of $NaGaGe_3Se_8$, $K_3Ga_3Ge_7S_{20}$, and $K_3Ga_3Ge_7Se_{20}$. A: $NaGaGe_3Se_8$, B: $K_3Ga_3Ge_7S_{20}$, C: $K_3Ga_3Ge_7Se_{20}$.

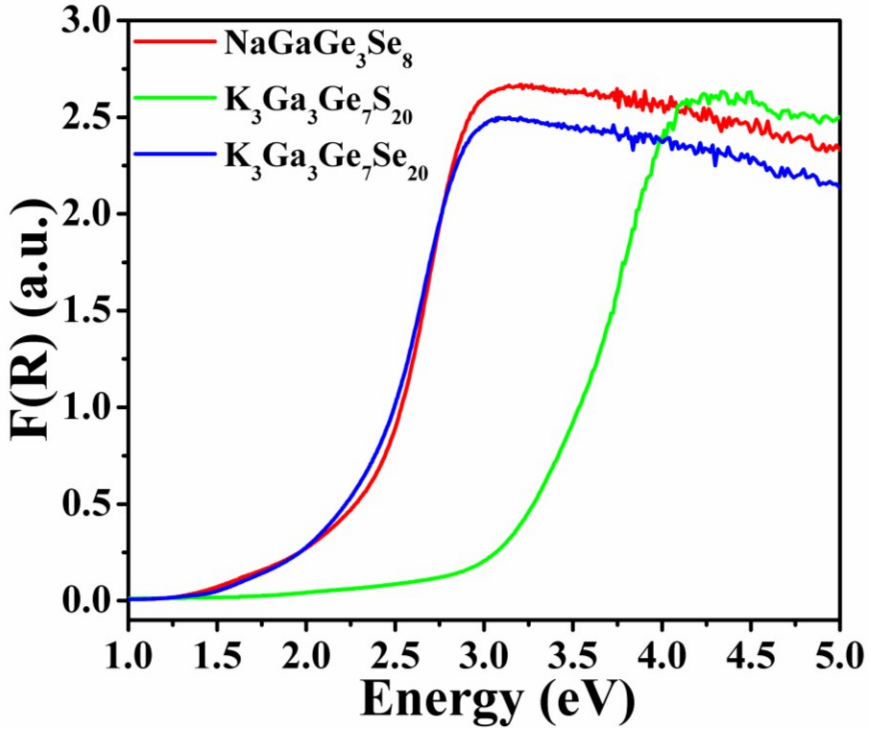

Fig. 4. Optical reflectance spectrum of $NaGaGe_3Se_8$, $K_3Ga_3Ge_7S_{20}$, and $K_3Ga_3Ge_7Se_{20}$.

Red: $NaGaGe_3Se_8$, Green: $K_3Ga_3Ge_7S_{20}$, Blue: $K_3Ga_3Ge_7Se_{20}$.

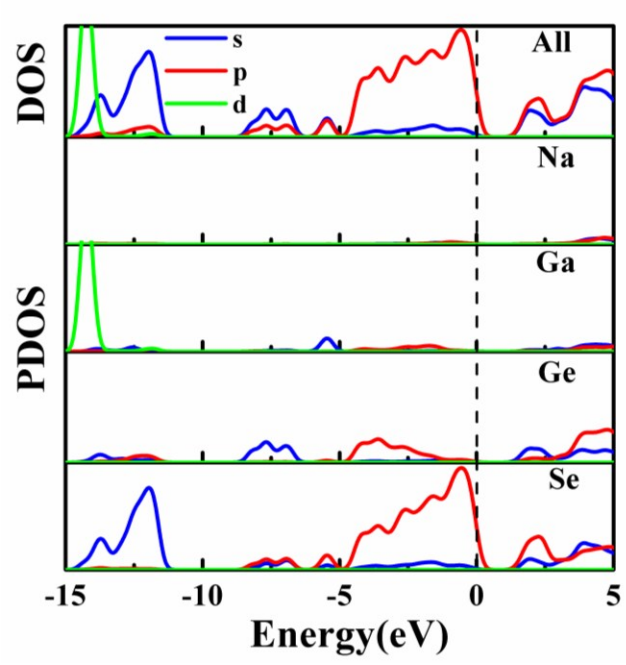

Fig. 5. The total and partial density of states (DOS and PDOS, respectively) of $NaGaGe_3Se_8$. Dashed line represents the Fermi energy (E_f).

Table of Contents Entry

$NaGaGe_3Se_8$ has a layered structure, while $K_3Ga_3Ge_7Q_{20}$ are constructed by the incompletely isolated quasi-2D layers, leading to large channels loosely occupied by K^+ cations.